Article

Never ending story? Biothermodynamic properties of biosynthesis and binding of Omicron BQ.1, BQ.1.1, XBB and XBB.1 variants of SARS-CoV-2

Marko Popovic*

School of Life Sciences, Technical University of Munich, Freising, Germany

*Correspondence: marko.popovic@tum.de or marko.popovic.td@gmail.com

Abstract: RNA viruses exhibit a great tendency to mutate. Starting from 2019, the wild type that was labeled Hu-1 has during the last 3 years evolved to produce several dozen new variants, as a consequence of mutations. Mutations cause changes in empirical formulas of new virus strains, which lead to change in thermodynamic properties of biosynthesis and binding. These changes cause changes in the rate of reactions of binding of virus antigen to the host cell receptor and the rate of virus multiplication in the host cell. Changes in thermodynamic and kinetic parameters lead to changes in biological parameters of infectivity and pathogenicity. SARS-CoV-2 has starting from in 2019, until today, evolved towards increase in infectivity and maintaining constant pathogenicity, or for some variants a slight decrease in pathogenicity. In the case of Omicron BQ.1, BQ.1.1, XBB and XBB.1 variants pathogenicity is identical as in the Omicron BA.2.75 variant. On the other hand, infectivity of the Omicron BQ.1, BQ.1.1, XBB and XBB.1 variants is greater than those of previous variants. This will most likely result in the phenomenon of asymmetric coinfection, that is circulation of several variants in the population, some being dominant.

Keywords: COVID-19; Elemental composition; Gibbs energy of biosynthesis; Gibbs energy of binding; Variant of concern (VOC)

---

1. Introduction

Viruses represent open thermodynamic systems [von Bertalanffy, 1950, 1971; Popovic and Minceva, 2020a; Şimşek et al., 2021]. Viruses have characteristic empirical formulas [Popovic and Minceva, 2020b; Degueldre, 2021], as well as thermodynamic properties of biosynthesis [Popovic, 2022a, 2022b, 2022c] and binding [Gale, 2022, 2021, 2020, 2019, 2018; Popovic and Popovic, 2022; Popovic, 2022d, 2022e, 2022f, 2022g]. Antigen-receptor binding represents a chemical reaction similar to protein-ligand interaction [Du et al., 2016; Popovic and Popovic, 2020]. Life processes - replication, transcription and translation represent chemical processes – polymerization of nucleotides into nucleic acid and amino acids into proteins [Pinheiro et al., 2008; Johansson and Dixon, 2013; Dodd et al., 2020; Lee et al., 2020]. Driving force for all chemical processes is Gibbs energy [Demirel, 2014; Balmer, 2010; Atkins and de Paula, 2011, 2014; von Stockar, 2013a, 2013b]. To understand biological processes, which have their chemical and biothermodynamic side, it is necessary to know the driving forces for these processes.

RNA viruses, including SARS-CoV-2, exhibit a great tendency to mutate [Duffy, 2018]. All variants of SARS-CoV-2, from Hu-1 to Omicron BA.2.75, have been chemically and thermodynamically characterized [Popovic and Popovic, 2022; Popovic, 2022a, 2022b, 2022c, 2022d, 2022e, 2022f, 2022g, Popovic and Minceva, 2021a, 2020b]. Change in thermodynamic properties of binding and biosynthesis during the time evolution of SARS-CoV-2 has been reported in [Popovic, 2022f].

During the last several months, the Omicron variant has developed new mutations, giving rise to new variants, including BQ.1, BQ.1.1 and XBB. These were labeled variants of concern (VOC) by WHO [2022]. The BA.2.75 and BQ.1 have been dominating lately [Zappa et al., 2022]. The question is raised whether they are competitive [Zappa et al., 2022]. Various viruses compete "for soil" [Popovic and Minceva, 2021a]. The result of this competition can be coinfection or interference [Popovic and Minceva, 2021a]. Experience learns us that newer variants have caused successive pandemic waves, suppressing the older variants [Popovic, 2022f].

The aim of this paper is to chemically and thermodynamically characterize the new BQ.1, BQ.1.1 and XBB variants and to compare their thermodynamic properties of biosynthesis and binding with other SARS-CoV-2 variants.

2. Methods

2.1 Data sources

The genetic sequences of the BQ.1, BQ.1.1, XBB and XBB.1 variants of SARS-CoV-2 were taken from GISAID, the global data science initiative [Khare et al., 2021; Elbe and Buckland-Merrett, 2017; Shu and McCauley, 2017]. The BQ.1 genetic sequence can be found under the accession ID: EPI_ISL_15921176. It is labeled as hCoV-19/Israel/ICH-741192169/2022. It has been collected on November 16, 2022 by a lab in Tel Aviv, Israel. The BQ.1.1 genetic sequence can be found under the accession ID: EPI_ISL_15938021. It is labeled hCoV-19/USA/MT-MTPHL-4070970/2022. It was isolated on November 23, 2022 by a lab in Helena, Montana (USA). The XBB genetic sequence can be found under the accession ID: EPI_ISL_15936982. It is labeled hCoV-19/Austria/LB-R00113-S325/2022. It was isolated on November 23, 2022 by a lab in Vienna, Austria. The XBB.1 genetic sequence can be found under the accession ID: EPI_ISL_15927855. It is labeled hCoV-19/Turkey/KSS-UEAH4881829747/2022. It was isolated on November 7, 2022 by a lab in Istanbul, Turkey. The findings of this study are based on metadata associated with 4 sequences available on GISAID up to December 2, 2022, and accessible at https://doi.org/10.55876/gis8.221202be.

The sequence of the nucleocapsid phosphoprotein of SARS-CoV-2 was obtained from the NCBI database [Sayers et al., 2022; National Center for Biotechnology Information, 2022], under the accession ID: UKQ14424.1. The number of copies of the nucleocapsid phosphoprotein in virus particle was taken from [Neuman and Buchmeier, 2016; Neuman et al., 2011; Neuman et al., 2006].

Dissociation equilibrium constants of the BQ.1, BQ.1.1, XBB, XBB.1, BA.2 and BA.4/5 variants were taken from Wang et al. [2022]. They were measured using surface plasmon resonance at 25°C [Wang et al., 2022; Rusnati et al., 2015].

Data on standard Gibbs energies of binding of the Wild type Hu-1, Alpha B.1.1.7, Beta B.1.351, Gamma P.1, Delta B.1.617 and Omicron BA.1 variants of SARS-CoV-2 were taken from [Popovic, 2022b]. All the data are at 25°C.

Data on standard Gibbs energies of biosynthesis of biosynthesis of the Hu-1, Delta B.1.617.2, Omicron BA.1.1.429, Omicron BA.2 and Omicron BA.2.75 variants of SARS-CoV-2 were taken from [Popovic, 2022a, 2022b, 2022c].

2.2 Empirical formulas and biosynthesis reactions

The genetic and protein sequences were used to find empirical formulas of nucleocapsids of the BQ.1, BQ.1.1 and XBB variants of SARS-CoV-2. This was done using the atom counting method [Popovic, 2022h]. The atom counting method is implemented using a computer program [Popovic, 2022h]. The input are genetic and protein sequences of the virus of interest, as well as the number of copies of proteins in the virus particle and the virus particle size [Popovic, 2022h]. The program goes along the nucleic acid and protein sequences and adds atoms coming from each residue in the sequence, to find the number of atoms contributed by that macromolecule to the virus particle [Popovic, 2022h]. The contributions of viral proteins are multiplied by their copy numbers, since proteins are present in multiple copies in virus particles [Popovic, 2022h]. The output of the program is elemental composition of virus particles, in the form of empirical formulas, and molar masses of virus particles [Popovic, 2022h]. The advantage of the atom counting method is that it can provide the empirical formulas of virus particles, based on widely available data on genetic and protein sequences [Popovic, 2022h]. The atom counting method was shown to give results in good agreement with experimental results [Popovic, 2022h].

The empirical formulas of virus particles were used to construct biosynthesis reactions, summarizing conversion of nutrients into new live matter [von Stockar, 2013a, 2013b; Battley, 1998]. The biosynthesis reaction for virus particles has the general form

$$\text{(Amino acid)} + O_2 + HPO_4^{2-} + HCO_3^{-} \longrightarrow \text{(Bio)} + SO_4^{2-} + H_2O + H_2CO_3 \qquad (1)$$

where (Bio) represents new live matter, described by an empirical formula given by the atom counting method [Popovic, 2022a, 2022b]. (Amino acid) represents a mixture of amino acids with the empirical formula $CH_{1.798}O_{0.4831}N_{0.2247}S_{0.022472}$ (expressed per mole of carbon), representing the source of energy, carbon, nitrogen and sulfur [Popovic, 2022a, 2022b]. O_2 is the electron acceptor [Popovic, 2022a, 2022b]. HPO_4^{2-} is the source of phosphorus [Popovic, 2022a, 2022b]. HCO_3^- is a part of the bicarbonate buffer that takes excess H^+ ions that are generated during biosynthesis [Popovic, 2022a, 2022b]. SO_4^{2-} is an additional metabolic product that takes excess sulfur atoms [Popovic, 2022a, 2022b]. H_2CO_3 takes the oxidized carbon atoms and is also a part of the bicarbonate buffer [Popovic, 2022a, 2022b].

2.3 Thermodynamic properties of live matter and biosynthesis

Empirical formulas of virus nucleocapsids were used to find standard thermodynamic properties of their live matter, using predictive biothermodynamic models: the Patel-Erickson and Battley equations [Patel and Erickson, 1981; Battley, 1999, 1998, 1992]. The Patel-Erickson equation was used to find enthalpy of live matter, based on its elemental composition. The Patel-Erickson equation gives standard enthalpy of combustion, $\Delta_C H^o$, of live matter

$$\Delta_C H^0(bio) = -111.14 \frac{kJ}{C\text{-}mol} \cdot E \qquad (2)$$

where E is number of electrons transferred to oxygen during combustion [Patel and Erickson, 1981; Battley, 1998, 1992; Popovic, 2019]. E can be calculated from the empirical formula of live matter

$$E = 4n_C + n_H - 2n_O - 0\, n_N + 5n_P + 6n_S \qquad (3)$$

where n_C, n_H, n_O, n_N, n_P and n_S represent the number of C, H, O, N, P and S atoms in the live matter empirical formula, respectively [Patel and Erickson, 1981; Battley, 1998, 1992; Popovic, 2019]. Once calculated using the Patel-Erickson equation, $\Delta_C H^o$ can be converted into standard entropy of formation, $\Delta_f H^o$, of live matter. $\Delta_C H^o$ is the enthalpy change of the reaction of complete combustion of live matter.

$C_{nC}H_{nH}O_{nO}N_{nN}P_{nP}S_{nS}$ + (n_C + ¼ n_H + 1¼ n_P + 1½ n_S - ½ n_O) O_2 → n_C CO_2 + ½ n_H H_2O + ½ n_N N_2 + ¼ n_P P_4O_{10} + n_S SO_3 (4)

This means that $\Delta_C H^o$ can be used to find $\Delta_f H^o$ of live matter using the equation, using the equation [Popovic, 2022b; Atkins and de Paula, 2011, 2014; Popovic, 2019]

$$\Delta_f H^0(bio) = n_C\, \Delta_f H^0(CO_2) + \frac{n_H}{2}\, \Delta_f H^0(H_2O) + \frac{n_P}{4}\, \Delta_f H^0(P_4O_{10}) + n_S\, \Delta_f H^0(SO_3) - \Delta_C H^0 \quad (5)$$

The Battley equation gives standard molar entropy of live matter, S^o_m, based on its empirical formula

$$S_m^0(bio) = 0.187\, \sum_J \frac{S_m^0(J)}{a_J} n_J \quad (6)$$

where n_J is the number of atoms of element J in the empirical formula of live matter [Battley, 1999; Battley and Stone, 2000; Popovic, 2019]. S^o_m and a_J are standard molar entropy and number of atoms per formula unit of element J in its standard state elemental form [Battley, 1999; Battley and Stone, 2000; Popovic, 2019]. The Battley equation can be modified to give standard entropy of formation, $\Delta_f S^o$, of live matter [Battley, 1999; Battley and Stone, 2000; Popovic, 2019]

$$S_m^0(bio) = -0.813\, \sum_J \frac{S_m^0(J)}{a_J} n_J \quad (7)$$

Finally, $\Delta_f H^o$ and $\Delta_f S^o$ are combined to give standard Gibbs energy of formation of live matter, $\Delta_f G^o$.

$$\Delta_f G^0(bio) = \Delta_f H^0(bio) - T\Delta_f S^0(bio) \quad (8)$$

Once live matter is characterized by finding its $\Delta_f H^o$, S^o_m and $\Delta_f G^o$, these properties can be combined with biosynthesis reactions to find standard thermodynamic properties of biosynthesis. Standard thermodynamic properties of biosynthesis include standard enthalpy of biosynthesis, $\Delta_{bs} H^o$, standard entropy of biosynthesis, $\Delta_{bs} S^o$, and standard Gibbs energy of biosynthesis, $\Delta_{bs} G^o$. These properties are found by applying the Hess's law to biosynthesis reactions

$$\Delta_{bs} H^0 = \sum_{products} \nu\, \Delta_f H^0 - \sum_{reactants} \nu\, \Delta_f H^0 \quad (9)$$

$$\Delta_{bs} S^0 = \sum_{products} \nu\, S_m^o - \sum_{reactants} \nu\, S_m^o \quad (10)$$

$$\Delta_{bs} G^0 = \sum_{products} \nu\, \Delta_f G^0 - \sum_{reactants} \nu\, \Delta_f G^0 \quad (11)$$

where ν represents a stoichiometric coefficient [Popovic, 2022b; Atkins and de Paula, 2011, 2014; von Stockar, 2013a, 2013b; Battley, 1998]. The most important of these three properties is standard Gibbs energy of biosynthesis, which represents the thermodynamic driving force for growth of all organisms [von Stockar, 2013a, 2013b; von Stockar and Liu, 1999], including viruses [Popovic, 2022b].

2.4 Thermodynamic properties of antigen-receptor binding

In order to multiply inside the cytoplasm, a virus must first enter its host cell. The first step in this process is binding of the virus antigen to the host cell receptor. The antigen of SARS-CoV-2 is the spike glycoprotein trimer (SGP) [Duan et al., 2020], while the host cell receptor is angiotensin-converting enzyme 2 (ACE2) [Scialo et al., 2020]. The process of antigen-receptor binding is, in its essence, a chemical reaction, similar to protein-ligand interactions [Du et al., 2016; Popovic and Popovic, 2022]. Thus, the binding of SGP to ACE2 can be described through the chemical reaction

(An) + (Re) = (An-Re)

Where (An) represents the virus antigen (SGP in the case of SARS-CoV-2), (Re) represents the host cell receptor (ACE2 for SARS-CoV-2), while (An-Re) represents the antigen-receptor complex [Du et al., 2016; Popovic and Popovic, 2022].

Like for all other chemical reactions, laws of chemical thermodynamics apply and the process of antigen-receptor binding can be described through several thermodynamic parameters. The dissociation equilibrium constant, K_d, is defined as

$$K_d = \frac{[An][Re]}{[An-Re]} \tag{12}$$

where [An] is the concentration of the virus antigen, [Re] the concentration of the host receptor and [An-Re] the concentration of the antigen-receptor complex [Du et al., 2016; Popovic and Popovic, 2022]. The reciprocal of K_d is the binding equilibrium constant, K_B, [Du et al., 2016; Popovic and Popovic, 2022]

$$K_B = \frac{1}{K_d} \tag{13}$$

The binding equilibrium constant can be used to find standard Gibbs energy of binding, $\Delta_B G^0$, through the equation

$$\Delta_B G^0 = -RT \ln K_B \tag{14}$$

Where T is temperature and R is the universal gas constant [Du et al., 2016; Popovic and Popovic, 2022].

3. Results

In this research, for the first time the empirical formula of BQ.1, BQ.1.1, XBB and XBB.1 variants of SARS-CoV-2 were calculated. They are given in Table 1. The empirical formula of the nucleocapsid of the BQ.1 variant is $CH_{1.574}O_{0.3427}N_{0.3124}P_{0.006027}S_{0.003358}$. The molar mass of the BQ.1 nucleocapsid empirical formula is 23.749 g/C-mol, while the molar mass of the entire BQ.1 nucleocapsid is 117.22 MDa. The empirical formula of nucleocapsid of the BQ.1.1 variant is $CH_{1.574}O_{0.3426}N_{0.3124}P_{0.006006}S_{0.003359}$. The molar mass of the BQ.1.1 nucleocapsid empirical formula is 23.747 g/C-mol, while the molar mass of the entire BQ.1.1 nucleocapsid is 117.28 MDa. The empirical formula of the nucleocapsid of the XBB variant is $CH_{1.574}O_{0.3427}N_{0.3124}P_{0.006028}S_{0.003358}$. The molar mass of the XBB nucleocapsid empirical formula is 23.749 g/C-mol, while the molar mass of the entire XBB nucleocapsid is 117.22 MDa. The empirical formula of the nucleocapsid of the XBB.1 variant is $CH_{1.574}O_{0.3426}N_{0.3124}P_{0.006012}S_{0.003359}$. The molar mass of the XBB.1 nucleocapsid empirical formula is 23.748 g/C-mol, while the molar mass of the entire XBB.1 nucleocapsid is 117.19 MDa.

Based on the empirical formulas of the SARS-CoV-2 variants, biosynthesis reactions were formulated. They are presented in Table 2. The biosynthesis reaction of the BQ.1 nucleocapsid is

$$1.3901\ CH_{1.798}O_{0.4831}N_{0.2247}S_{0.022472} + 0.4913\ O_2 + 0.0060\ HPO_4^{2-} + 0.0437\ HCO_3^{-} \longrightarrow CH_{1.574}O_{0.3427}N_{0.3124}P_{0.006027}S_{0.003358} + 0.0279\ SO_4^{2-} + 0.0538\ H_2O + 0.4338\ H_2CO_3 \qquad (1)$$

The biosynthesis reaction of the BQ.1.1 nucleocapsid is

$$1.3900\ CH_{1.798}O_{0.4831}N_{0.2247}S_{0.022472} + 0.4911\ O_2 + 0.0060\ HPO_4^{2-} + 0.0437\ HCO_3^{-} \longrightarrow CH_{1.574}O_{0.3426}N_{0.3124}P_{0.006006}S_{0.003359} + 0.0279\ SO_4^{2-} + 0.0538\ H_2O + 0.4337\ H_2CO_3 \qquad (2)$$

The biosynthesis reaction of the XBB nucleocapsid is

$$1.3901\ CH_{1.798}O_{0.4831}N_{0.2247}S_{0.022472} + 0.4913\ O_2 + 0.0060\ HPO_4^{2-} + 0.0437\ HCO_3^{-} \longrightarrow CH_{1.574}O_{0.3427}N_{0.3124}P_{0.006028}S_{0.003358} + 0.0279\ SO_4^{2-} + 0.0538\ H_2O + 0.4338\ H_2CO_3 \qquad (3)$$

The biosynthesis reaction of the XBB.1 nucleocapsid is

$$1.3900\ CH_{1.798}O_{0.4831}N_{0.2247}S_{0.022472} + 0.4912\ O_2 + 0.0060\ HPO_4^{2-} + 0.0437\ HCO_3^{-} \longrightarrow CH_{1.574}O_{0.3426}N_{0.3124}P_{0.006012}S_{0.003359} + 0.0279\ SO_4^{2-} + 0.0538\ H_2O + 0.4337\ H_2CO_3 \qquad (4)$$

Standard thermodynamic properties of live matter of nucleocapsids of the BQ.1, BQ.1.1, XBB and XBB.1 variants were calculated and are shown in Table 3. Standard enthalpy of formation of the BQ.1 nucleocapsid is -75.40 kJ/C-mol, its standard molar entropy is 32.49 J/C-mol K, while its standard Gibbs energy of formation is -33.28 kJ/C-mol. Standard enthalpy of formation of the BQ.1.1 nucleocapsid is -75.38 kJ/C-mol, its standard molar entropy is 32.49 J/C-mol K, while its standard Gibbs energy of formation is -33.26 kJ/C-mol. Standard enthalpy of formation of the XBB nucleocapsid is -75.40 kJ/C-mol, its standard molar entropy is 32.49 J/C-mol K, while its standard Gibbs energy of formation is -33.28 kJ/C-mol. Finally, standard enthalpy of formation of the XBB.1 nucleocapsid is -75.38 kJ/C-mol, its standard molar entropy is 32.49 J/C-mol K, while its standard Gibbs energy of formation is -33.26 kJ/C-mol.

In this research, for the first time the Gibbs energy of biosynthesis is calculated for BQ.1, BQ.1.1, XBB and XBB.1 variants of SARS-CoV-2. They are presented in Table 4. Standard enthalpy of biosynthesis of the BQ.1 nucleocapsid is -232.33 kJ/C-mol, its standard entropy of biosynthesis is -37.34 J/C-mol K, while its standard Gibbs energy of biosynthesis is -221.24 kJ/C-mol. Standard enthalpy of biosynthesis of the BQ.1.1 nucleocapsid is -232.27 kJ/C-mol, its standard entropy of biosynthesis is -37.33 J/C-mol K, while its standard Gibbs energy of biosynthesis is -221.18 kJ/C-mol. Standard enthalpy of biosynthesis of the XBB nucleocapsid is -232.34 kJ/C-mol, its standard entropy of biosynthesis is -37.34 J/C-mol K, while its standard Gibbs energy of biosynthesis is -221.25 kJ/C-mol. Finally, standard enthalpy of biosynthesis of the XBB.1 nucleocapsid is -232.28 kJ/C-mol, its standard entropy of biosynthesis is -37.33 J/C-mol K, while its standard Gibbs energy of biosynthesis is -221.19 kJ/C-mol.

Based on K_d data reported in Wang et al. [2022], standard thermodynamic properties of antigen-receptor binding have been determined for BQ.1, BQ.1.1, XBB, XBB.1, BA.2 and BA.4/5 variants of SARS-CoV-2. They are given in Table 5 and include the binding equilibrium constant, K_B, and standard Gibbs energy of binding, $\Delta_B G^o$. For the BQ.1 variant, the binding equilibrium constant is $K_B = 1.613 \times 10^9\ M^{-1}$, while the standard Gibbs energy of antigen-receptor binding is $\Delta_B G^o = -52.55$ kJ/mol. For the BQ.1.1 variant, the binding equilibrium constant is $K_B = 1.786 \times 10^9\ M^{-1}$, while the standard Gibbs energy of antigen-receptor binding is $\Delta_B G^o = -52.81$ kJ/mol. For the XBB variant, the binding equilibrium constant is $K_B = 5.000 \times 10^8\ M^{-1}$, while the standard Gibbs energy of antigen-receptor binding is $\Delta_B G^o = -49.65$ kJ/mol. For the XBB.1 variant, the binding equilibrium constant is $K_B = 4.854 \times 10^8\ M^{-1}$, while the standard Gibbs energy of antigen-receptor binding is $\Delta_B G^o = -49.58$ kJ/mol. For the BA.2 variant, the binding equilibrium constant is $K_B = 1.053 \times 10^9$ M^{-1}, while the standard Gibbs energy of antigen-receptor binding is $\Delta_B G^o = -51.50$ kJ/mol. For the BA.4/5 variants, the binding equilibrium constant is $K_B = 1.639 \times 10^9$ M^{-1}, while the standard Gibbs energy of antigen-receptor binding is $\Delta_B G^o = -52.59$ kJ/mol.

Table 1: Empirical formulas of nucleocapsids of the BQ.1, BQ.1.1, XBB and XBB.1 variants of SARS-CoV-2. The empirical formulas have the general form $C_{nC}H_{nH}O_{nO}N_{nN}P_{nP}S_{nS}$. All formulas are expressed per mole of carbon. Molar masses are provided in two forms. *Mr* denotes the molar mass of the empirical formula and is expressed in g/C-mol (Daltons). *Mr*(*nc*) denotes the molar mass of the entire nucleocapsid (entire viral genome and all nucleoprotein copies) and is expressed in MDa.

Variant	C	H	O	N	P	S	Mr (g/C-mol)	Mr(nc) (MDa)
BQ.1 nucleocapsid	1	1.574	0.3427	0.3124	0.006027	0.003358	23.749	117.22
BQ.1.1 nucleocapsid	1	1.574	0.3426	0.3124	0.006006	0.003359	23.747	117.18
XBB nucleocapsid	1	1.574	0.3427	0.3124	0.006028	0.003358	23.749	117.22
XBB.1 nucleocapsid	1	1.574	0.3426	0.3124	0.006012	0.003359	23.748	117.19

Table 2: Biosynthesis reactions of the BQ.1, BQ.1.1, XBB and XBB.1 variants of SARS-CoV-2.

Variant	Reactants					Products			
	Amino acid	O_2	HPO_4^{2-}	HCO_3^-	→	Bio	SO_4^{2-}	H_2O	H_2CO_3
BQ.1 nucleocapsid	1.3901	0.4913	0.0060	0.0437	→	1	0.0279	0.0538	0.4338
BQ.1.1 nucleocapsid	1.3900	0.4911	0.0060	0.0437	→	1	0.0279	0.0538	0.4337
XBB nucleocapsid	1.3901	0.4913	0.0060	0.0437	→	1	0.0279	0.0538	0.4338
XBB.1 nucleocapsid	1.3900	0.4912	0.0060	0.0437	→	1	0.0279	0.0538	0.4337

Table 3: Standard thermodynamic properties of live matter for the analyzed SARS-CoV-2 variants. This table presents standard enthalpy of formation, $\Delta_f H^o$, standard molar entropy, S^o_m, and standard Gibbs energy of formation, $\Delta_f G^o$, at 25°C (298.15 K).

Variant	$\Delta_f H^o$ (kJ/C-mol)	S^o_m (J/C-mol K)	$\Delta_f G^o$ (kJ/C-mol)
BQ.1 nucleocapsid	-75.40	32.49	-33.28
BQ.1.1 nucleocapsid	-75.38	32.49	-33.26
XBB nucleocapsid	-75.40	32.49	-33.28
XBB.1 nucleocapsid	-75.38	32.49	-33.26

Table 4: Standard thermodynamic properties of biosynthesis for the analyzed SARS-CoV-2 variants. This table gives data on standard enthalpy of biosynthesis, $\Delta_{bs} H^o$, standard entropy of biosynthesis, $\Delta_{bs} S^o$, and standard Gibbs energy of biosynthesis, $\Delta_{bs} G^o$, at 25°C (298.15 K).

Variant	$\Delta_{bs} H^o$ (kJ/C-mol)	$\Delta_{bs} S^o$ (J/C-mol K)	$\Delta_{bs} G^o$ (kJ/C-mol)
BQ.1 nucleocapsid	-232.33	-37.34	-221.24
BQ.1.1 nucleocapsid	-232.27	-37.33	-221.18

XBB nucleocapsid	-232.34	-37.34	-221.25
XBB.1 nucleocapsid	-232.28	-37.33	-221.19

Table 5: Standard thermodynamic properties of antigen-receptor binding of SARS-CoV-2 variants. This table shows data on dissociation equilibrium constants, K_d, binding equilibrium constants, K_B, and standard Gibbs energies of binding, $\Delta_B G^0$. All the data are at 25°C (298.15 K). The K_d data were taken from Wang et al. [2022].

Variant	K_d (M)	K_B (M^{-1})	$\Delta_B G^0$ (kJ/mol)
BQ.1	6.2E-10	1.613E+09	-52.55
BQ.1.1	5.6E-10	1.786E+09	-52.81
XBB	2E-09	5.000E+08	-49.65
XBB.1	2.06E-09	4.854E+08	-49.58
BA.2	9.5E-10	1.053E+09	-51.50
BA.4/5	6.1E-10	1.639E+09	-52.59

4. Discussion

Zappa et al. [2022] have asked an interesting question: will the new Omicron variants compete with the currently dominant BA.2.75 variant. Having in mind that viruses are biological, chemical and thermodynamic entities and that during their life cycle they perform chemical reactions (binding, replication, transcription and translation), this means that they compete for resources. The rate of the mentioned chemical reactions, according to the phenomenological equations, which belong to nonequilibrium thermodynamics, directly depends on Gibbs energy of the process [Popovic and Popovic, 2022]. Indeed, the rate of binding, r_B, is given by the phenomenological equation

$$r_B = -\frac{L_B}{T}\Delta_B G \tag{4}$$

where $\Delta_B G$ is the Gibbs energy of binding, T is temperature, while L_B is the binding phenomenological coefficient [Popovic and Popovic, 2022; Popovic, 2022b, 2022g]. Furthermore, the rate of biosynthesis, r_{bs}, of viral components is given by the biosynthesis phenomenological equation

$$r_{bs} = -\frac{L_{bs}}{T}\Delta_{bs} G \tag{5}$$

where $\Delta_{bs} G$ is the Gibbs energy of biosynthesis, while L_{bs} is the biosynthesis phenomenological coefficient [Popovic, 2022a, 2022b, 2022c]. Through analysis of the two phenomenological equations, it is possible to predict the outcome of competition of two viruses, if they appear at the same time in the same place and compete for the same population. If Gibbs energies of binding are approximately same, then the result of competition will be coinfection [Popovic and Minceva, 2021a]. Furthermore, if Gibbs energies of biosynthesis are similar, the result of competition will be coinfection [Popovic and Minceva, 2021a]. However, if Gibbs energies of binding and biosynthesis are slightly different, the result will be asymmetric coinfection [Popovic and Minceva, 2021a]. Asymmetric coinfection means that both variants will appear in the population, but one of them, the one characterized by a more negative Gibbs energy of binding and biosynthesis, will dominate [Popovic and Minceva, 2021a]. A large difference in Gibbs energies of binding and/or biosynthesis will lead to the phenomenon of interference [Popovic and Minceva, 2021a].

In this paper, standard Gibbs energies of biosynthesis were determined for BQ.1 (-221.24 kJ/C-mol), BQ.1.1 (-221.18 kJ/C-mol) and XBB (-221.25 kJ/C-mol). Gibbs energy of biosynthesis for the BA.2.75 subvariant is -221.18 kJ/C-mol [Popovic, 2022a]. From these data, we can conclude that in case of competition there is no winner, that all the variants multiply at the same rate, leading to coinfection, since they all have similar Gibbs energies of biosynthesis.

The next interesting question is related to pathogenicity of the new variants. Pathogenicity is related to the rate of multiplication of viruses. Greater multiplication rate leads to greater damage to host cells [Popovic, 2022f]. Greater damage to host cells is a good indicator of virus pathogenicity. Gibbs energies of biosynthesis of viral components for the BA.2.75, BQ.1, BQ.1.1 and XBB variants are approximate the same. Thus, the multiplication rate of the new variants is approximately equal to the multiplication rate of BA.2.75, which leads to the conclusion that the pathogenicity of the new variants is identical to that of BA.2.75. Figure 1 shows a graphical representation of time evolution of SARS-CoV-2, including the new BQ.1, BQ.1.1 and XBB variants. The graph shows that Gibbs energies of biosynthesis of BA.2.75 and the new variants differ on the second decimal. This difference is negligible and is not sufficient to show the difference in pathogenicity. The Omicron variant has evolved towards maintaining constant multiplication rate and pathogenicity.

Infectivity depends on the affinity of antigen-receptor binding, and the rate of virus binding and entry into host cells, according to the binding phenomenological equation (4). Gibbs energy of binding is the driving force for the reaction of antigen-receptor binding [Popovic and Popovic, 2022; Popovic, 2022b, 2022d]. Gibbs energy of binding for the Omicron BA.2.75 variant is −49.41 kJ/mol [Popovic, 2022g]. In this research, standard Gibbs energies of binding were found to be: -52.55 for the BQ.1 variant, -52.81 kJ/mol for the BQ.1.1 variant, -49.65 kJ/mol for the XBB variant and -49.58 kJ/mol for the XBB.1 variant. The XBB and XBB.1 variants have very similar standard Gibbs energies of binding to BA.2.75, meaning that they will have an almost identical entry rates. However, BQ.1 and BQ.1.1 have slightly more negative Gibbs energy of binding that BA.2.75. This implies that the entry rates of BQ.1 and BQ.1.1 into host cells will be greater than that of BA.2.75. Having in mind that the difference in Gibbs energies of binding is not great, in case of simultaneous circulation of Omicron BA.2.75, BQ.1 and BQ.1.1 variants, in the population, there will be asymmetric coinfection.

SARS-CoV-2 has continued to evolve in the direction it has taken since the beginning of the COVID-19 pandemic, related to slight increase in infectivity with maintaining pathogenicity at a relatively constant level. Thus, it is not possible to give a definite response to the question of the time of arrival of the pandemic phase “game over”.

Figure 2 shows the time evolution of Gibbs energy of binding of SARS-CoV-2. From the graph, a trend can be observed towards a more negative Gibbs energy of binding of new variants. As was extrapolated in the paper [Popovic, 2022f], new mutations on the receptor binding domain (RBD) have developed towards increase in binding affinity. The mutations have led to change in elemental composition and empirical formulas, which characterize the new variants. Change in empirical formulas have led to changes in thermodynamic properties of new variants, in the exact direction predicted by the theory of evolution.

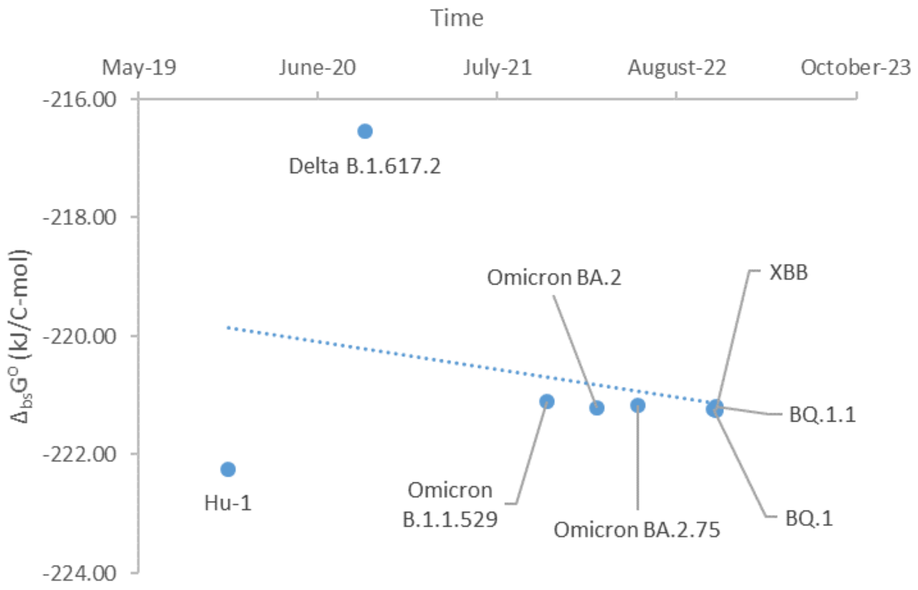

Figure 1: Time evolution of SARS-CoV-2 variants through standard Gibbs energies of biosynthesis. This time shows standard Gibbs energy of biosynthesis, $\Delta_{bs}G^0$, of various SARS-CoV-2 variants, which appeared at different times.

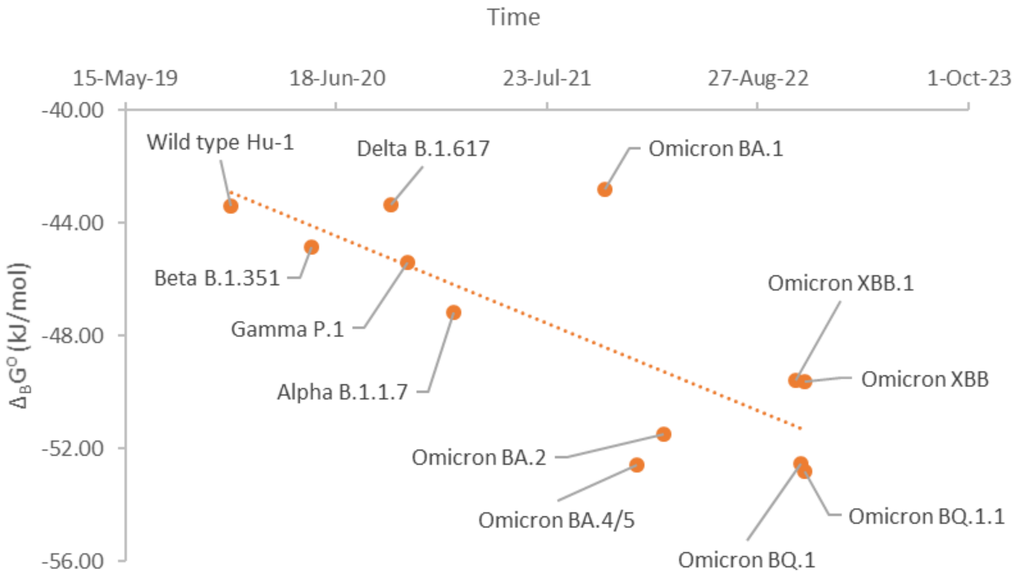

Figure 2: Time evolution of SARS-CoV-2 variants through standard Gibbs energies of binding. This time shows standard Gibbs energy of binding, $\Delta_B G^0$, of various SARS-CoV-2 variants, which appeared at different times.

5. Conclusions

Empirical formulas and molar masses have been determined for the nucleocapsids of BQ.1, BQ.1.1 and XBB virions. The empirical formula of the BQ.1 nucleocapsid is $CH_{1.574}O_{0.3427}N_{0.3124}P_{0.006027}S_{0.003358}$. For the BQ.1.1 nucleocapsid the empirical formula is $CH_{1.574}O_{0.3426}N_{0.3124}P_{0.006006}S_{0.003359}$. For the XBB nucleocapsid, the empirical formula is $CH_{1.574}O_{0.3427}N_{0.3124}P_{0.006028}S_{0.003358}$. The molar mass of the BQ.1 nucleocapsid empirical formula is 23.749 g/C-mol, while the molar mass of the entire BQ.1 nucleocapsid is 117.22 MDa. The molar mass of the BQ.1.1 nucleocapsid empirical formula is 23.747 g/C-mol, while the molar mass of the entire BQ.1.1 nucleocapsid is 117.28 MDa. The molar mass of the XBB nucleocapsid empirical formula is 23.749 g/C-mol, while the molar mass of the entire XBB nucleocapsid is 117.22 MDa.

Thermodynamic properties of biosynthesis BQ.1, BQ.1.1 and XBB variants differ very little from those of other Omicron variants. Thus, pathogenicity of new variants has not changed compared to BA.2.75.

New variants that compete with BA.2.75 should exhibit the phenomenon of coinfection. Several variants can simultaneously circulate in the population, causing a new wave of the pandemic.

The BQ.1, BQ.1.1 variants have evolved towards more negative standard Gibbs energy of binding, leading to increase in infectivity. This is in agreement with the expectation of the evolution theory and empirical observations.

Supplementary Materials: The following are available online.

Acknowledgements: The author gratefully acknowledges all data contributors, i.e., the Authors and their Originating laboratories responsible for obtaining the specimens, and their Submitting laboratories for generating the genetic sequence and metadata and sharing via the GISAID Initiative, on which this research is based.

Conflicts of Interest: The authors declare no conflict of interest.”

References

Atkins, P. W., & de Paula, J. (2011). *Physical Chemistry for the Life Sciences (2nd edition)*, W. H. Freeman and Company. ISBN-13: 978-1429231145

Atkins, P.W. & de Paula, J. (2014). *Physical Chemistry: Thermodynamics, Structure, and Change, 10th Edition*. New York: W. H. Freeman and Company. ISBN-13: 978-1429290197

Balmer, R.T. (2010). *Modern Engineering Thermodynamics*, Cambridge, MA: Academic Press. https://doi.org/10.1016/C2009-0-20199-1

Battley, E. H., & Stone, J. R. (2000). A comparison of values for the entropy and the entropy of formation of selected organic substances of biological importance in the solid state, as determined experimentally or calculated empirically. *Thermochimica acta*, *349*(1-2), 153-161. https://doi.org/10.1016/S0040-6031(99)00509-2

Battley, E.H. (1999). An empirical method for estimating the entropy of formation and the absolute entropy of dried microbial biomass for use in studies on the thermodynamics of microbial growth. *Thermochimica Acta*, 326(1-2), 7-15. https://doi.org/10.1016/S0040-6031(98)00584-X

Battley, E. H. (1998). The development of direct and indirect methods for the study of the thermodynamics of microbial growth. *Thermochimica Acta*, *309*(1-2), 17-37. https://doi.org/10.1016/S0040-6031(97)00357-2

Battley, E.H. (1992). On the enthalpy of formation of Escherichia coli K-12 cells, *Biotechnology and Bioengineering,* 39, 5-12. https://doi.org/10.1002/bit.260390103

Degueldre, C. (2021). Single virus inductively coupled plasma mass spectroscopy analysis: A comprehensive study. *Talanta*, *228*, 122211. https://doi.org/10.1016/j.talanta.2021.122211

Demirel, Y. (2014). *Nonequilibrium Thermodynamics: Transport and Rate Processes in Physical, Chemical and Biological Systems, 3rd ed*. Amsterdam: Elsevier. ISBN: 9780444595812

Dodd, T., Botto, M., Paul, F. et al. (2020). Polymerization and editing modes of a high-fidelity DNA polymerase are linked by a well-defined path. *Nat Commun* 11, 5379. https://doi.org/10.1038/s41467-020-19165-2

Du, X., Li, Y., Xia, Y. L., Ai, S. M., Liang, J., Sang, P., ... & Liu, S. Q. (2016). Insights into protein–ligand interactions: mechanisms, models, and methods. *International journal of molecular sciences*, *17*(2), 144. https://doi.org/10.3390/ijms17020144

Duan, L., Zheng, Q., Zhang, H., Niu, Y., Lou, Y., & Wang, H. (2020). The SARS-CoV-2 Spike Glycoprotein Biosynthesis, Structure, Function, and Antigenicity: Implications for the Design of Spike-Based Vaccine Immunogens. *Frontiers in immunology*, *11*, 576622. https://doi.org/10.3389/fimmu.2020.576622

Duffy S. (2018). Why are RNA virus mutation rates so damn high?. *PLoS biology*, *16*(8), e3000003. https://doi.org/10.1371/journal.pbio.3000003

Elbe, S. and Buckland-Merrett, G. (2017) Data, disease and diplomacy: GISAID's innovative contribution to global health. Global Challenges, 1:33-46. doi: 10.1002/gch2.1018 PMCID: 31565258

Gale P. (2022). Using thermodynamic equilibrium models to predict the effect of antiviral agents on infectivity: Theoretical application to SARS-CoV-2 and other viruses. *Microbial risk analysis*, *21*, 100198. https://doi.org/10.1016/j.mran.2021.100198

Gale P. (2021). Using thermodynamic equilibrium models to predict the effect of antiviral agents on infectivity: Theoretical application to SARS-CoV-2 and other viruses. Microbial risk analysis, 100198. Advance online publication. https://doi.org/10.1016/j.mran.2021.100198

Gale P. (2020). How virus size and attachment parameters affect the temperature sensitivity of virus binding to host cells: Predictions of a thermodynamic model for arboviruses and HIV. *Microbial risk analysis*, *15*, 100104. https://doi.org/10.1016/j.mran.2020.100104

Gale P. (2019). Towards a thermodynamic mechanistic model for the effect of temperature on arthropod vector competence for transmission of arboviruses. *Microbial risk analysis*, *12*, 27–43. https://doi.org/10.1016/j.mran.2019.03.001

Gale P. (2018). Using thermodynamic parameters to calibrate a mechanistic dose-response for infection of a host by a virus. *Microbial risk analysis*, *8*, 1–13. https://doi.org/10.1016/j.mran.2018.01.002

Johansson, E., & Dixon, N. (2013). Replicative DNA polymerases. *Cold Spring Harbor perspectives in biology*, *5*(6), a012799. https://doi.org/10.1101/cshperspect.a012799

Khare, S., et al (2021) **GISAID's Role in Pandemic Response**. *China CDC Weekly*, 3(49): 1049-1051. doi: 10.46234/ccdcw2021.255 PMCID: 8668406

Lee, J., Schwarz, K. J., Kim, D. S., Moore, J. S., & Jewett, M. C. (2020). Ribosome-mediated polymerization of long chain carbon and cyclic amino acids into peptides in vitro. *Nature communications*, *11*(1), 4304. https://doi.org/10.1038/s41467-020-18001-x

National Center for Biotechnology Information (2022). NCBI Database [online]. Available at: https://www.ncbi.nlm.nih.gov/ (Accessed on December 2, 2022).

Neuman, B.W. and Buchmeier, M.J. (2016). Supramolecular architecture of the coronavirus particle. *Advances in Virus Research*, 96, 1-27. https://doi.org/10.1016/bs.aivir.2016.08.005

Neuman, B. W., Kiss, G., Kunding, A. H., Bhella, D., Baksh, M. F., Connelly, S., Droese, B., Klaus, J. P., Makino, S., Sawicki, S. G., Siddell, S. G., Stamou, D. G., Wilson, I. A., Kuhn, P., & Buchmeier, M. J. (2011). A structural analysis of M protein in coronavirus assembly and morphology. *Journal of structural biology*, *174*(1), 11–22. https://doi.org/10.1016/j.jsb.2010.11.021

Neuman, B. W., Adair, B. D., Yoshioka, C., Quispe, J. D., Orca, G., Kuhn, P., Milligan, R. A., Yeager, M., & Buchmeier, M. J. (2006). Supramolecular architecture of severe acute respiratory syndrome coronavirus revealed by electron cryomicroscopy. *Journal of virology*, *80*(16), 7918–7928. https://doi.org/10.1128/JVI.00645-06

Patel, S.A. and Erickson, L.E. (1981). Estimation of heats of combustion of biomass from elemental analysis using available electron concepts. *Biotechnology and Bioengineering,* 23, 2051-2067. https://doi.org/10.1002/bit.260230910

Pinheiro, A. V., Baptista, P., & Lima, J. C. (2008). Light activation of transcription: photocaging of nucleotides for control over RNA polymerization. *Nucleic acids research*, *36*(14), e90. https://doi.org/10.1093/nar/gkn415

Popovic, M. and Popovic, M. (2022). Strain Wars: Competitive interactions between SARS-CoV-2 strains are explained by Gibbs energy of antigen-receptor binding. *Microbial Risk Analysis*. https://doi.org/10.1016/j.mran.2022.100202

Popovic, M. (2022a). Omicron BA.2.75 Sublineage (Centaurus) Follows the Expectations of the Evolution Theory: Less Negative Gibbs Energy of Biosynthesis Indicates Decreased Pathogenicity. *Microbiology Research*, *13*(4), 937–952. MDPI AG. Retrieved from http://dx.doi.org/10.3390/microbiolres13040066

Popovic M. (2022b). Strain wars 3: Differences in infectivity and pathogenicity between Delta and Omicron strains of SARS-CoV-2 can be explained by thermodynamic and kinetic parameters of binding and growth. *Microbial risk analysis*, 100217. Advance online publication. https://doi.org/10.1016/j.mran.2022.100217

Popovic, M. (2022c). Strain Wars 4 - Darwinian evolution through Gibbs' glasses: Gibbs energies of binding and growth explain evolution of SARS-CoV-2 from Hu-1 to BA.2. *Virology.* https://doi.org/10.1016/j.virol.2022.08.009

Popovic, M. (2022d). Strain wars 2: Binding constants, enthalpies, entropies, Gibbs energies and rates of binding of SARS-CoV-2 variants. *Virology*, 570, 35-44. https://doi.org/10.1016/j.virol.2022.03.008

Popovic, M. (2022e). Strain Wars 5: Gibbs energies of binding of BA.1 through BA.4 variants of SARS-CoV-2. *Microbial Risk Analysis*. https://doi.org/10.1016/j.mran.2022.100231

Popovic, M. (2022f). Beyond COVID-19: Do biothermodynamic properties allow predicting the future evolution of SARS-CoV-2 variants?. *Microbial risk analysis*, *22*, 100232. https://doi.org/10.1016/j.mran.2022.100232

Popovic, M. (2022g). Omicron BA.2.75 Subvariant of SARS-CoV-2 Is Expected to Have the Greatest Infectivity Compared with the Competing BA.2 and BA.5, Due to Most Negative Gibbs Energy of Binding. *BioTech*, *11*(4), 45. MDPI AG. Retrieved from http://dx.doi.org/10.3390/biotech11040045

Popovic M. (2022h). Atom counting method for determining elemental composition of viruses and its applications in biothermodynamics and environmental science. *Computational biology and chemistry*, *96*, 107621. https://doi.org/10.1016/j.compbiolchem.2022.107621

Popovic, M., & Minceva, M. (2021a). Coinfection and Interference Phenomena Are the Results of Multiple Thermodynamic Competitive Interactions. *Microorganisms*, *9*(10), 2060. https://doi.org/10.3390/microorganisms9102060

Popovic, M., & Minceva, M. (2020a). A thermodynamic insight into viral infections: do viruses in a lytic cycle hijack cell metabolism due to their low Gibbs energy?. *Heliyon*, *6*(5), e03933. https://doi.org/10.1016/j.heliyon.2020.e03933

Popovic, M., & Minceva, M. (2020b). Thermodynamic insight into viral infections 2: empirical formulas, molecular compositions and thermodynamic properties of SARS, MERS and SARS-CoV-2 (COVID-19) viruses. *Heliyon*, 6(9), e04943. https://dx.doi.org/10.1016%2Fj.heliyon.2020.e04943

Rusnati, M., Chiodelli, P., Bugatti, A., & Urbinati, C. (2015). Bridging the past and the future of virology: surface plasmon resonance as a powerful tool to investigate virus/host interactions. *Critical reviews in microbiology*, *41*(2), 238–260. https://doi.org/10.3109/1040841X.2013.826177

Sayers, E. W., Bolton, E. E., Brister, J. R., Canese, K., Chan, J., Comeau, D. C., Connor, R., Funk, K., Kelly, C., Kim, S., Madej, T., Marchler-Bauer, A., Lanczycki, C., Lathrop, S., Lu, Z., Thibaud-Nissen, F., Murphy, T., Phan, L., Skripchenko, Y., Tse, T., … Sherry, S. T. (2022). Database resources of the national center for biotechnology information. *Nucleic acids research*, *50*(D1), D20–D26. https://doi.org/10.1093/nar/gkab1112

Scialo, F., Daniele, A., Amato, F., Pastore, L., Matera, M. G., Cazzola, M., Castaldo, G., & Bianco, A. (2020). ACE2: The Major Cell Entry Receptor for SARS-CoV-2. *Lung*, *198*(6), 867–877. https://doi.org/10.1007/s00408-020-00408-4

Shu, Y. and McCauley, J. (2017) GISAID: from vision to reality. EuroSurveillance, 22(13) doi: 10.2807/1560-7917.ES.2017.22.13.30494 PMCID: PMC5388101

Şimşek, B., Özilgen, M., & Utku, F. Ş. (2021). How much energy is stored in SARS-CoV-2 and its structural elements?. *Energy Storage*, e298. https://doi.org/10.1002/est2.298

Von Bertalanffy, L. (1950). The theory of open systems in physics and biology. *Science*, 111(2872), 23-29. https://doi.org/10.1126/science.111.2872.23

Von Bertalanffy, L. (1971). *General System Theory: Foundations, Development, Applications*. New York, NY: George Braziller Inc. ISBN-13: 978-0807604533

Von Stockar, U. (2013a). Live cells as open non-equilibrium systems. In Urs von Stockar, ed., *Biothermodynamics: The Role of Thermodynamics in Biochemical Engineering*, Lausanne: EPFL Press, 475-534. https://doi.org/10.1201/b15428

Von Stockar, U. (2013b). Biothermodynamics of live cells: energy dissipation and heat generation in cellular structures. In: *Biothermodynamics: the role of thermodynamics in Biochemical Engineering*, von Stockar, U., ed., Lausanne: EPFL Press, pp. 475-534. https://doi.org/10.1201/b15428

von Stockar, U., & Liu, J. (1999). Does microbial life always feed on negative entropy? Thermodynamic analysis of microbial growth. *Biochimica et biophysica acta*, *1412*(3), 191–211. https://doi.org/10.1016/s0005-2728(99)00065-1

Wang, Q., Iketani, S., Li, Z., Liu, L., Guo, Y., Huang, Y., ... & Ho, D. D. (2022). Alarming antibody evasion properties of rising SARS-CoV-2 BQ and XBB subvariants. *bioRxiv*, 2022.11.23.517532. https://doi.org/10.1101/2022.11.23.517532

WHO (2022). TAG-VE statement on Omicron sublineages BQ.1 and XBB. [Online] World Health Organization. Available at: https://www.who.int/news/item/27-10-2022-tag-ve-statement-on-omicron-sublineages-bq.1-and-xbb (Accessed on November 29, 2022)

Zappa, M., Verdecchia, P., & Angeli, F. (2022). The new phase of pandemic: Are BA.2.75 and BQ.1 competitive variants? An in silico evaluation. *European journal of internal medicine*, S0953-6205(22)00389-2. Advance online publication. https://doi.org/10.1016/j.ejim.2022.11.006